ISBN: 978-3-95450-219-6 ISSN: 2226-0366 doi: 10.18429/JACoW-LINAC2024-MOPB036

ACCELERATING STRUCTURES FOR THE FCC-ee PRE-INJECTOR COMPLEX: RF DESIGN, OPTIMIZATION, AND PERFORMANCE ANALYSIS

A. Kurtulus, A. Grudiev, A. Latina, CERN, Geneva, Switzerland
S. Bettoni, P. Craievich, J.-Y. Raguin, Paul Scherrer Institut, Villigen, Switzerland

Abstract

The Future Circular Collider electron-positron (FCC-ee) pre-injector complex demands high-performance RF accelerating structures to achieve reliable and efficient acceleration of beams up to 20 GeV. In this study, we describe an analytical approach to RF design for the traveling-wave (TW) structures including a pulse compression system to meet the rigorous specifications of the FCC-ee pre-injector complex. The fundamental mode at 2.8 GHz and Higher Order Mode (HOM) characteristics were determined through the utilization of lookup tables and analytical formulas, enabling efficient exploration of extensive parameter ranges. Optimization of the structure geometry and in particular the iris parameters was performed to address key challenges including maximizing effective shunt impedance, minimizing surface fields, and effectively damping long-range wakes through HOM detuning. Moreover, we investigated the impact of beam-loading effects on the bunch-to-bunch energy spread. Comprehensive thermal and mechanical analyses were carried out to evaluate the impact on the accelerating structure performance during operation at a repetition frequency of 100 Hz.

INTRODUCTION

The proposed new baseline for the FCC-ee injector complex [1] includes an updated high-energy linear accelerator (HE linac). This design enhancement increases the number of bunches per RF pulse from two to four while reducing the repetition rate to 100 Hz. Each bunch will have a charge of 5 nC, an rms length of 1 mm, and a bunch spacing of 25 ns.

The following section provides an update on the RF design, optimization, and performance analysis, including the methodology and specific structural features of the HE linac.

RF DESIGN METHODOLOGY

A parametric study was conducted to optimize accelerator structure design. Lookup tables were generated to rapidly assess the impact of aperture radius a and iris thickness d on the first twenty HOMs of a convex cell at the synchronous frequencies. The primary design goal was to enhance shunt impedance relative to previous S-band structures [2]. The target structure was defined by an RF frequency of 2.8 GHz, RF phase advance ψ of 120° per cell, and a length L_s of 3 meters. An average aperture of 0.12λ [3] (equivalent to 12.85 mm) was selected as a suitable compromise between beam dynamics and RF considerations. The long-range transverse wake is damped through the detuning of dipole modes, eliminating the necessity for additional damping elements. This is accomplished by tapering the aperture and iris thickness while maintaining an average aperture of 0.12λ. The design constraint requires that the transverse wakefield potential W_t remains at or below 0.1 V/pC/mm/m within the time range of 25 to 100 ns.

A SLED-type [4] RF pulse compressor was analytically designed and implemented to further optimize the performance. This device increases the peak amplitude of the RF pulses and shortens their duration by storing energy in a cavity and then releasing it in a compressed form. The resultant boost in peak RF power significantly impacts the electric field strength within the accelerator cavities, which is essential for achieving the target acceleration gradients. Consequently, the effective shunt impedance $R_{\text{eff}} = \langle G(t = T_k)\rangle^2 L_s/P_k$ (where $\langle G(t = T_k)\rangle$ is the average gradient at beam injection, L_s is the length of the structure, and P_k is the klystron power), which measures the efficiency of RF power transfer to the beam, was carefully evaluated.

OPTIMIZATION OF THE RF STRUCTURE

A parametric sweep was conducted to optimize the HE linac RF structure design based on shunt impedance calculations. Using a lookup table, iris thicknesses ranging from 2.04 mm to 6.2 mm were tested to maximize shunt impedance.

To assess tapering effects, the delta Δ parameter was introduced as an offset relative to the constant aperture structure, adjusting the first and last cell apertures while maintaining a linear variation between them. Positive delta values resulted in down-tapering (larger first cell aperture, smaller last cell), and negative values led to up-tapering. Delta was varied from -4 mm to 4 mm in 0.2 mm steps, and the highest shunt impedance was identified. Finally, a wakefield analysis was conducted using frequency-domain parameters of 20 lowest HOMs, with designs selected based on analytically calculated wakefields that remain below 0.1 V/pC/mm/m, refining the linac's aperture and iris thickness for optimal performance.

Figure 1 presents the results of a parametric sweep of maximum effective shunt impedance as a function of the delta parameter. The red traces depict the effective shunt impedance values under conditions where transverse wakefields are not constrained, providing a baseline for comparison. In contrast, the blue traces illustrate the effective shunt impedance when the transverse wakefield is limited to a threshold of 0.1 V/pC/mm/m. We observed that a delta of 2 mm achieves the highest effective shunt impedance while meeting wakefield constraints and exhibiting a low surface electric field

ISBN: 978-3-95450-219-6 ISSN: 2226-0366 doi: 10.18429/JACoW-LINAC2024-MOPB036

that is highlighted with a yellow star on Fig. 1, leading us to select this configuration as the candidate structure for HE linac. Following the identification of the optimal configuration with a delta of 2 mm, we proceeded to calculate the corresponding structure parameters.

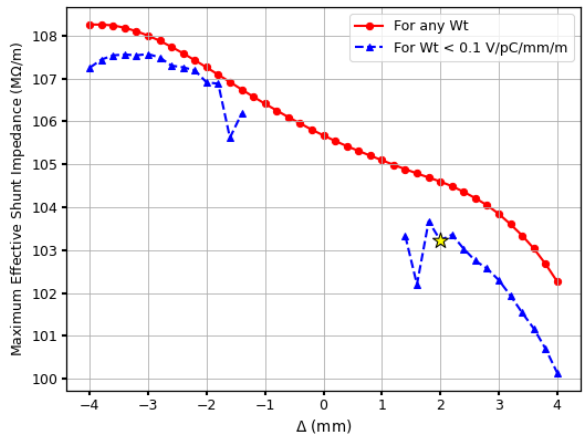

Figure 1: Parametric sweep of effective shunt impedance as a function of delta Δ. Red traces show results without transverse wakefield constraints, while blue traces indicate conditions with a 0.1 V/pC/mm/m wakefield threshold.

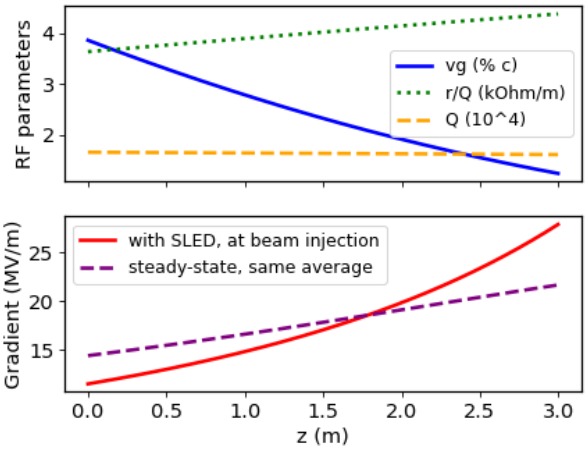

Figure 2: RF parameters are shown in the top subplot, while the bottom subplot illustrates gradient variations along the structure.

The detailed values are presented together with the key parameters of the SLED-type RF pulse compressor in Table 1. Additionally, Fig. 2 offers a detailed visual depiction of the RF parameters and gradient change throughout the structure, giving a comprehensive view of how these variables vary along the structure.

For more realistic wakefield results, we utilized the ECHO2D [5] time-domain solver, where we model all 84 cells of the structure and accounts for an infinite number of HOMs together with coupling between the cells, yielding more accurate long-range wakefield predictions. To rigorously analyze worst-case scenarios and long-range wakefield effects, we employed the envelope-of-the-envelope approach on the wakefield data that is calculated by ECHO2D code and lookup table. The results are shown on Fig. 3. The analysis reveals that a bunch spacing of 25 ns with 4 bunches is practical, given that the wakefield levels remain below the threshold within the range of 25 ns to 100 ns.

Table 1: Specifications of the HE Linac Structures

Parameter	Value
Frequency	2.8 GHz
Average aperture	0.12λ
RF phase advance	$2\pi/3$
Length (# cells)	3.0 m (84)
Tapered aperture	14.85 mm → 10.85 mm
Tapered iris thickness	2.84 mm → 4.04 mm
Filling time	460 ns
Klystr. power per structure	15 MW
Eff. shunt impedance	102 MΩ/m
Average gradient	22.5 MV/m
Repetition rate	100 Hz
Avg. Structure input power	3.9 kW
Max. instant. E	41 MV/m
Max. instant. S_c	161 MV/μm^2
SLED coupling	15
SLED unloaded Q factor	200000
Klystr. pulse length	3 μs

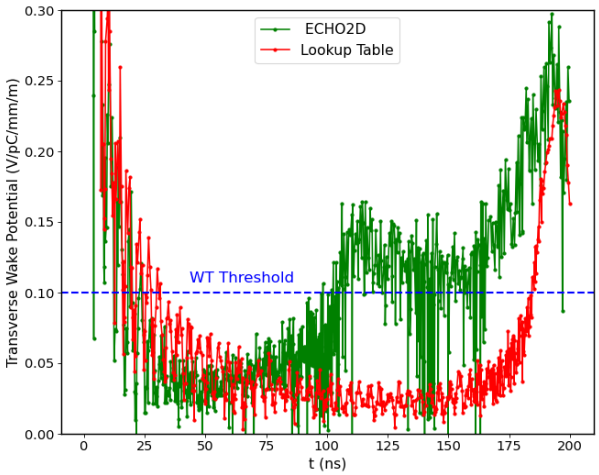

Figure 3: Envelope-of-the-envelope of transverse wakefield potentials for the HE linac structure, calculated over time using both the Lookup Table and ECHO2D methods.

THERMO-MECHANICAL STUDIES

A steady-state thermal model of the last cell in the HE linac structure, which has the highest average wall losses, was created using the CST [6] thermal solver. Magnetic field data from the electromagnetic solver were used to calculate surface power dissipation and imported into the thermal model. The model included eight cooling channels, each

ISBN: 978-3-95450-219-6 ISSN: 2226-0366 doi: 10.18429/JACoW-LINAC2024-MOPB036

16 mm in diameter, with a convection coefficient of 4000 W/m^2/K, based on a water flow rate of 4.4 L/min per channel and a water temperature of 293 K. Assuming an average RF output power of 2.39 kW, corresponding to a 100 Hz repetition rate for a 3 µs pulse with a peak power of 15 MW, and accounting for an attenuation factor of 0.87 from the pulse compressor and 0.61 from the accelerating structure, the temperature distribution was calculated and shown in Fig. 4. The model demonstrates that the peak temperature occurs in the iris region, which is 0.28°C higher than the initial condition. Based on thermal studies we simulated total deformation on the last cell with the mechanical solver of ANSYS [7] which showed maximum deformation of 0.06 µm, which is negligible.

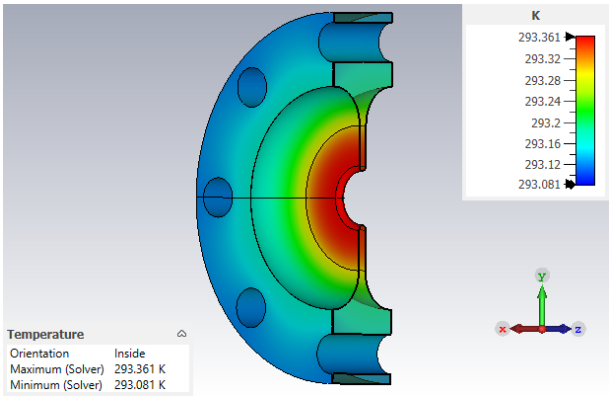

Figure 4: Temperature distribution of the first cell of HE linac structure.

BEAM-LOADING STUDIES

The beam loading effect is analyzed under the assumption of a constant beam current of 0.2 A, corresponding to a bunch charge of 5 nC with a bunch separation of 25 ns and a total of 4 bunches. Normalizing the beam voltage with the maximum unloaded voltage in Fig. 5 enables a precise evaluation of beam-loading effects and helps in understanding the impact of these effects on the energy variation between bunches. As anticipated, the highest energy variation is observed in the fourth bunch, measuring 2.42%.

Modulating the klystron input pulse shape effectively reduces bunch-to-bunch energy variation. Our study specifically explores the application of a step-like function to the RF input signal to achieve this reduction. By leveraging the known parameters of klystron pulse length, filling time, and bunch separation, we can precisely adjust either unloaded or loaded voltages. While this paper focuses on the unloaded voltage case, the same modulation technique is also effective for managing loaded voltage variations. The step-like modulated normalized klystron input amplitude is shown in Fig. 6. By appropriately adjusting the amplitude values for each step, we successfully achieved a flattening of the unloaded voltage, with the total bunch-to-bunch energy variation observed to be less than 0.1%.

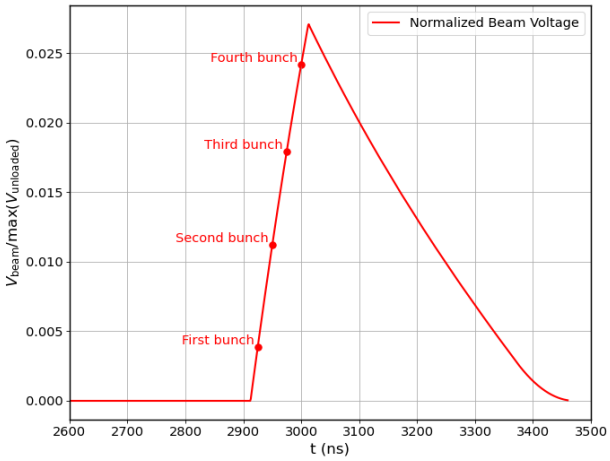

Figure 5: Distribution of the beam voltage for the four bunches, normalized to the maximum unloaded voltage.

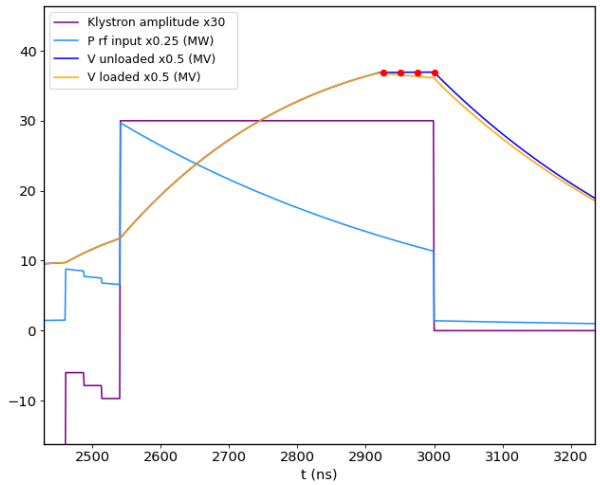

Figure 6: Minimization of bunch-to-bunch energy variation of unloaded voltage by applying step-like modulated klystron input pulse.

CONCLUSION

This study presents a successful design and optimization of RF accelerating structures for the FCC-ee pre-injector complex, achieving key performance goals including a shunt impedance of 102 MΩ/m and a stable acceleration gradient of 22.5 MV/m. The use of a SLED-type pulse compressor and precise iris tuning have minimized transverse wakefields and thermal stress, ensuring structural integrity with a minimal temperature rise of 0.28°C. Additionally, we studied beam-loading effects, reducing energy spread between bunches to less than 0.1% by modulating the klystron input pulse shape. These results demonstrate the efficiency of our RF design approach in addressing the challenges posed by the FCC-ee pre-injector complex and provide a robust foundation for future developments in high-energy linear accelerators.

ISBN: 978-3-95450-219-6 ISSN: 2226-0366 doi: 10.18429/JACoW-LINAC2024-MOPB036

REFERENCES

[1] P. Craievich, "Injector complex: status and outlook", presented at the FCC Week 2024, San Francisco, United States, Jun. 2024. https://indico.cern.ch/event/1298458/contributions/5977869/.

[2] H. W. Pommerenke *et al.*, "RF design of traveling-wave accelerating structures for the FCC-ee pre-injector complex", in *Proc. LINAC'22*, Liverpool, UK, Aug.-Sep. 2022, pp. 707–710. doi:10.18429/JACoW-LINAC2022-THPOJO08

[3] S. Bettoni *et al.*, "High bunch charge linacs design for FCC-ee project", presented at IPAC'24, Nashville, TN, 2024, paper MOPC45, unpublished.

[4] Z. D. Farkas, H. A. Hogg, G. A. Loew, and P. B. Wilson, "SLED: A method of doubling SLAC's energy", in *Proc. 9th Int. Conf. On High Energy Accelerators*, SLAC, Stanford, CA, USA, May 1974, pp. 576–583.

[5] I. Zagorodnov, K. L. Bane, and G. Stupakov, "Calculation of wakefields in 2d rectangular structures", *Phys. Rev. Spec. Top. Accel. Beams*, vol. 18, no. 10, p. 104 401, 2015. doi:10.1103/PhysRevSTAB.18.104401

[6] CST Studio Suite, version 2024.02, Dassault Systèmes, 2024. https://www.3ds.com/products-services/simulia/products/cst-studio-suite/

[7] ANSYS Inc., *ANSYS Mechanical: Thermo-Mechanical Solver*, version v2024.1, 2024. https://www.ansys.com/products/structures/ansys-mechanical